Journal of Applied Polymer Science

Influence of process parameters on the structure formation of man-made cellulosic fibers from ionic liquid solution

Anne Michud, Michael Hummel, Herbert Sixta
Department of Forest Products Technology, Aalto University, School of Chemical Technology, P.O. 16300, 00076 Aalto, Espoo, Finland
Correspondence to: H. Sixta (E-mail: herbert.sixta@aalto.fi)

ABSTRACT: The influence of dry-jet wet spinning parameters on the production of man-made cellulosic fibers from 13 wt % cellulose/1,5-diazabicyclo[4.3.0]non-5-ene acetate solutions was investigated. The spinneret nozzle diameter, extrusion velocity, draw ratio, and coagulation bath temperature were the studied parameters. The production of highly oriented fibers was favored by selecting higher extrusion velocity and lower spinneret diameter. A spinneret size of 100 μm and a draw ratio of 6 were sufficient to highly orient the cellulose macromolecules and achieve tenacities above 40 cN/tex (600 MPa). Total orientation assessed via birefringence measurement, tenacity, and Young's modulus values reached a plateau at a draw of 6 and no further development in properties was observed. A temperature of the aqueous coagulation bath of 15 °C slightly promoted greater orientation of the fibers by hampering structural changes of the cellulose macromolecules in the nascent solid fibers. Furthermore, the determination of the elongational viscosity of the liquid thread via the measurement of radial force tensor was tested and showed promising results. © 2016 Wiley Periodicals, Inc. J. Appl. Polym. Sci. **2016**, *133*, 43718.

KEYWORDS: mechanical properties; morphology; rubber; viscosity and viscoelasticity

Received 18 January 2016; accepted 1 April 2016
DOI: 10.1002/app.43718

INTRODUCTION

The world population has significantly increased during the past 10 years and is estimated to reach 8.3 billion by 2030. This growth has a tremendous impact on the worldwide demand for consumer goods which also includes fibers for various textile applications. The improvement of material prosperity and health standards, particularly in the developing countries, considerably contributes to the augmentation in fiber demand.[1,2]

In 2014, the total fiber consumption rose by 4.1% to 93.7 million tons of which 39.1% were cellulosic fibers [natural and man-made cellulosic fibers (MMCFs)]. MMCFs represent the most ideal substitute for cotton as they demonstrate wearability properties similar to cotton that cannot be met adequately by synthetic fibers.[1,2]

MMCFs have undergone many developments since their first appearance in the 1850s. The viscose and Lyocell fibers are currently the two main types of MMCFs present in the market. The viscose process which was developed in the late 19th century is still the largest industrial source of MMCFs despite the well-known environmentally unfriendly aspects of their manufacture.[3,4] The Lyocell process, employing the environmentally friendly solvent *N*-methylmorpholine *N*-oxide (NMMO), emerged in the early 1990s as an alternative to the viscose process.[5–7] However, some aspects of the Lyocell process, such as the thermal instability of the solvent and the high steam consumption required for the recovery of the large amount of water used in the process, remain problematic.[8,9]

Ionic liquids (ILs), which consist entirely of anions and cations, have been developed and thoroughly investigated during the past decades as direct solvent for cellulosic materials.[10–14] Their low melting point, low vapor pressure, and thermal stability render them attractive for industrial processes. IL spinning appears to be a promising substitute to the Lyocell-NMMO process as it is based on the same dry-jet wet spinning technology but offers safer processing conditions.[9,15,16]

The Ioncell-F(iber) is a recently developed method intended as an alternative to the currently commercialized viscose and Lyocell processes for the production of MMCFs.[16–18] The Ioncell-F technology, which employs a non-imidazole based IL as cellulose solvent, is also classified as a Lyocell-type process according to BISFA (International Bureau for the standardization of Rayon and Synthetic Fibres, Brussels) as it utilizes the same

Additional Supporting Information may be found in the online version of this article.

dry-jet wet spinning technique as the Lyocell-NMMO system. In the Ioncell-F, cellulose is first dissolved in 1,5-diazabicyclo[4.3.0]non-5-ene acetate ([DBNH]OAc) without any derivatization. The resulting polymer solution is then extruded at mild temperature through a spinneret via an air gap into an aqueous coagulation bath. The fluid filaments, which are drawn in the air gap immediately after the extrusion, are collected as continuous filaments and typically converted into staple fibers for further conversion into textile yarns. The formation of fibers by dry-jet wet spinning from cellulose/IL solution follows complex mechanisms, which need to be understood to establish a steady fiber production. The polymer solution is subjected to various deformation and flow conditions during the process such as shear and extensional stresses in the spinneret capillaries and in the air gap, respectively. In the latter, the fluid filaments undergo several changes such as relaxation, drawing, and cooling, which directly affect the formation of the structure of the cellulose network. The subsequent coagulation of the filament in the aqueous precipitation bath involves some structural modifications as well.[19] The process parameters such as spinneret geometry, extrusion velocity, draw ratio, and coagulation bath temperature all influence significantly the generation of the molecular structure of the fibers by modifying the flows and stresses present in the different shaping zones.

Spinnability of polymer solutions, which can be defined as the ability of a fluid filament to receive irreversible deformation without failure when subjected to uniaxial stress,[20] is closely related to the chosen process parameters and the rheological properties of the fluid filament in the air gap. Fundamental studies to determine the adequate conditions for continuous spinning and to define the relationships between the manufacturing process conditions and the properties of the final product are thus required.

The influence of the process parameters on the molecular structure and mechanical properties of NMMO-Lyocell fibers has been thoroughly investigated in a series of publications by Mortimer *et al.* In a first study, the effect of the draw ratio, line speed, and spinneret diameter were examined through the diameter and birefringence profile of the extruded filament in the air gap as well as the determination of the modulus and tenacity of the dry fibers.[21] The overall evolution of the filament structure from the spinneret surface to the dry fiber was presented in a second paper by studying the diameter and birefringence profiles through the spinning process.[19] The influence of the air gap conditions on the evolution of the filament structure was assessed in a third paper which demonstrated the significant impact of the air gap length, temperature, and humidity on the structure formation process.[22] In contrast, only few studies on the influence of process parameters on the structure formation of IL-based fibers have been conducted. One of the few, Jiang *et al.*, investigated the influence of the spinning speed on the structure and mechanical properties of fibers spun from cellulose/1-butyl-3-methylimidazolium chloride solution. They demonstrated that higher spinning speed leads to greater orientation and crystallinity resulting in higher tenacity and initial modulus of the regenerated cellulose fibers.[23]

In this study, a selected number of important spinning parameters are investigated to establish their effect on the structure formation of the cellulose network and on the mechanical properties of the resulting Ioncell-fibers. This work focuses on the nozzle diameter, extrusion velocity, draw ratio, elongational viscosity in the air gap, and coagulation bath temperature. The influence of these parameters on the total orientation and thus on the mechanical properties of the dry fibers is studied through the measurement of the filament diameter, the determination of the birefringence, and the tensile properties of the resulting fibers.

EXPERIMENTAL

Raw Material

Birch (*Betula pendula*) prehydrolysis kraft pulp ($[\eta] = 476$ mL/g, DP = 1133, $M_n = 65.9$ kDa, $M_w = 269.3$ kDa, polydispersity index 4.1, Enocell Speciality Cellulose, Finland) was used as cellulosic solute. The pulp was delivered in sheet form and cut to a powder by means of a Wiley mill. The intrinsic viscosity of the pulp was determined in cupriethylenediamine (CED) according to the standard method SCAN-CM 15:99. The pulp molar mass distribution was characterized by gel permeation chromatography employing lithium chloride/*N,N*-dimethylacetamide as solvent and pullulan standards for calibration. The GPC-system consisted of a pre-column (PLgel Mixed-A, 7.5 × 50 mm), four analytical columns (4 × PLgel Mixed-A, 7.5 × 300 mm) and a RI-detector (Shodex RI-101). After a solvent exchange sequence, to remove the residual water and activate the sample in *N,N*-dimethylacetamide, the samples were dissolved in 90 g/L LiCl/DMAc at room temperature under constant slow speed magnetic stirring. The dissolved cellulose samples were then diluted in pure DMAc to reach a concentration of 1 mg/mL in 9 g/L LiCl/DMAc. Filtration with 0.2 µm syringe filter was carried out and a volume of 100 µL was separated at 25 °C at a flow rate of 0.750 mL/min with 9 g/L LiCl/DMAc as eluent. Pullulan standards with molecular weights ranging from 343 Da to 708,000 Da were selected for the calibration. A correction of the molar mass distribution obtained by direct-standard-calibration was done with an algorithm calculating cellulose-equivalent molar masses of pullulan standards ($MM_{cellulose} = q \times MM^{p}_{pullulan}$, with $q = 12.19$ and $p = 0.78$) as suggested by Berggren *et al.* and Borrega *et al.*[24,25]

[DBNH]OAc Synthesis

[DBNH]OAc was synthesized by adding an equimolar amount of acetic acid (glacial, 100%, Merck, Germany) to 1,5-diazabicyclo[4.3.0]non-5-ene, DBN, (99%, Fluorochem, UK). Both components were used as received. The addition was performed carefully under external cooling due to the exothermic nature of the reaction. After complete addition of the required amount of acid, the solution was further stirred for 1 h at 80 °C.

Preparation of Cellulose/[DBNH]OAc Solution

About 13 wt % cellulose solutions were prepared for this study. Birch prehydrolysis kraft pulp was dissolved in [DBNH]OAc by means of a vertical kneader at 80 °C. The cellulose/[DBNH]OAc mixture was first homogenized manually before being transferred to the pre-heated vertical kneader.[26] Temperature, torque moment, vacuum, and revolution per min (rpm) were recorded

online. A dissolution time of 60 min at 10 rpm, 80 °C, and vacuum of 100 mbar was sufficient for complete cellulose dissolution which was verified by means of polarized light optical microscopy. Subsequently, the solutions were filtered via a hydraulic pressure filtration unit (1–2 MPa, metal filter fleece, 5–6 μm absolute fineness, Gebr. Kufferath AG, Germany) to remove any impurities or un-dissolved particles and assure constant solution quality during spinning. The resulting gel-like solutions were shaped according to the dimension of the spinning cylinder and solidified within 1–2 days after preparation.

Rheological Characterization

The visco-elastic behavior of cellulose/[DBNH]OAc solutions were investigated by means of an Anton Paar MCR 300 rheometer with a plate and plate geometry (25 mm diameter, 1 mm gap size) by conducting oscillatory measurements. The visco-elastic domain was first defined by dynamic strain sweep tests and a strain of 0.5% was selected for the subsequent frequency tests. The latter were performed over an angular frequency range, ω, of 0.01–100 s^{-1} at temperatures from 70 to 90 °C. Complex viscosity, η^*, and the storage, G', and loss, G'', moduli were recorded. The zero shear viscosity, η_0, was determined by fitting the complex viscosity data to the three-parameter Cross viscosity model given by eq. (1).[27] The Cox–Merz rule is here assumed to be valid.[28]

$$\eta = \frac{\eta_0}{\left[1+(\tau\dot{\gamma})^{1-n}\right]} \quad (1)$$

where τ is a time constant and n is the power-law exponent.

Dry-Jet Wet Spinning of Cellulose/[DBNH]OAc

Fibers were spun with a customized laboratory dry-jet wet piston spinning unit (Fourné Polymertechnik, Germany), simplified in Figure 1. The spinning cylinder was first charged with the solid [DBNH]OAc solution and then heated to the spinning temperature to yield a homogeneous spinnable solution. The spinning temperatures were selected according to the rheological behavior of the polymer solutions in order to be located in a specific matrix in which the spinnability of [DBNH]OAc solutions is guaranteed.[29] Spinning temperatures were set between 75 and 85 °C. The extrusion velocity, draw ratio, coagulation bath temperature, and spinneret diameter were the process parameters under investigation in this study. Air gap distance (1 cm), immersion depth to the first deflection roller (37 cm), deflection angle, and the retention distance of the filament bundle in the coagulation bath were kept constant throughout all spinning trials. The assessment of the extensional viscosity required the variation of the air gap distance and was varied from 1 to 4.5 cm. An overview of the experiments and the respective parameter sets are given in Table I. The maximum draw ratio, DR (ratio of take-up velocity/extrusion velocity), which is a measure of the elongation applied on the cellulose filament, is reported for each experiment and reflects the spinnability of [DBNH]OAc solutions. The maximum DR was determined by increasing slowly the velocity of the take-up godet until filament breaches occurred. The reported DRs correspond to the range of draw ratios in which no breaks of the cellulose filaments were observed for a minimum of 3 min. The extrusion velocity of the spinning unit can be set from 0.8 to 5 cm^3/min (2.8–17.7 m/min) and the take-up velocity is limited to 100 m/min.

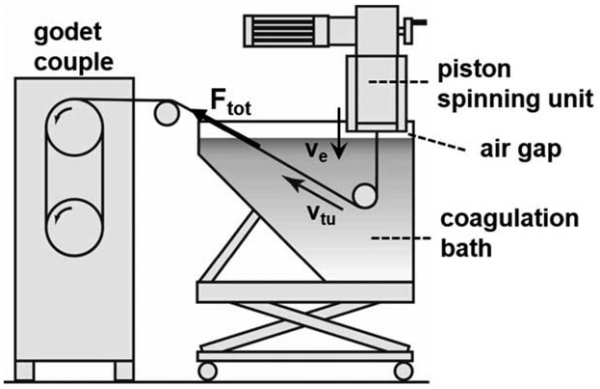

Figure 1. Schematic illustration of the dry-jet wet spinning unit employed for the production of cellulosic fibers.

Radial force Measurement for Elongational Viscosity Determination

The elongational viscosity of the fluid filament, which is here considered constant in the air gap, is determined by assessing the total force acting on the bundle of filaments when exiting the coagulation bath (see Figure 1) as a function of reciprocal air gap length. The total force after the bath is considered to be composed of the rheological (F_{rheo}) and the hydrodynamical force (F_{hydr}), given by eq. (2).[30]

$$F_{tot} = F_{rheo} + F_{hydr} \quad (2)$$

The filament velocity is defined by an exponential profile when only the external and rheological forces are considered in the force balance acting on the fluid filament in the air gap.[30]

$$v_1 = v_0 \exp\left(\frac{F_{rheol}}{Q\eta_e}\right) \quad (3)$$

By combining eqs. (2) and (3), the elongational viscosity is calculated from the slope of the plot of F_{tot} versus the reciprocal air gap length, as shown in eq. (4).[30]

$$F_{tot} = \frac{Q\eta_e}{l}\ln\left(\frac{V_1}{V_0}\right) + F_{hydr} \quad (4)$$

where Q is the throughput outflow, V_0, the extrusion velocity and V_1 the take-up velocity.

F_{tot} is measured by means of a strain gauge based force sensor placed at the exit of the coagulation bath. The measuring principle is based on the evaluation of the forces acting radially onto the sensor. The load transmission is effected through the pulley which is mounted onto the sensor's bearing journal. The force balance and detailed calculations of F_{tot} are reported in the Supporting Information.

Characterization of the Spun Fibers

Tensile Test. The quality of the resulting fibers was assessed using two Lenzing Instrument devices (Vibroskop and Vibrodyn 400). The fibers were characterized in terms of linear density (dtex), tenacity (cN/tex), and elongation at break (%) at conditioned state (23 °C, 50% humidity). Ten fibers per sample were tested. The tensile measurements comprise a gauge length of

Table I. Process Parameter Matrix

Spinneret geometry	Extrusion velocity (m/min)	Coagulation bath temperature (°C)	DR	Air gap (cm)
36 μm × 100 μm, *L*/*D*[a] 0.2	3.5	15	1.5–25.0	1
		12	1.5	1–3.5
	5.7	15	1.5–15.0	1
		20	1.5–15.0	1
		23	1.5–15.0	1
		12	1.5	1–3.5
36 μm × 150 μm, *L*/*D* 0.2	3.5	15	1.5–20.1	1
	5.2	12	1.5	1.5–4.5
36 μm × 200 μm, *L*/*D* 0.2	3.5	15	1.5–12.0	1

[a] Length/diameter ratio of the spin capillary.

20 mm, pretension 5.9 ± 1.2 mN/tex, and a speed of 20 mm/min according to DIN 53816. The Young's modulus of the spun fibers was calculated using a Matlab program determining the slope of the entire elastic region of the stress–strain curves obtained from the tensile tests according to ASTM standard D2256/D2256M.

Birefringence Measurement. The orientation of the cellulose chains of the spun fibers was determined by means of a polarized light microscope (Zeiss Axio Scope) equipped with a 5λ Berek compensator. The birefringence, Δn, of the fibers was obtained by dividing the retardation of the polarized light by the thickness of the fiber which was calculated from the linear density using a cellulose density value of 1.5 g/cm^3.[3] The total orientation factor f_t was determined by dividing Δn by the maximum birefringence of cellulose 0.062.[31]

RESULTS AND DISCUSSION

Influence of the Draw Ratio and Linear Extrusion Velocity

The solution is extruded through the spinneret orifices before entering the aqueous coagulation bath via an air gap. A preorientation of the molecule chains is first created in the spinneret capillaries due to the shear deformation that forces the cellulose chains to align in flow direction. However, this prealignment diminishes as the fluid experiences abrupt changes in the shear field when leaving the capillary. An immediate relaxation of the cellulose chains occurs at the exit of the spinneret which attenuates the orientation created by the spinneret flow.[20] The extent of this phenomenon, which is reflected in an increase of the fluid filament diameter at the exit of the spinneret, depends on the spinneret geometry, extrusion velocity, and in particular on the viscoelastic properties of the extruded solution. This so-called die swell can be over-compensated in the air gap by the elongational flow created when drawing the filament.[21] The main orientation of the polymer chains occurs thus in the air gap between the spinneret and the surface of the precipitation bath due to the drawing process. The effect of the drawing process on the thickness of the fluid filament, total orientation of the cellulose chains, and mechanical properties of the spun fibers is exhibited in Figures 2 and 3. In the air gap, the titer or thickness of the spun filaments is reduced when applying higher stretching on the spun filaments. This is in agreement with an earlier study by Hauru *et al.* in which they define a correlation between the titer and the draw ratio.[32] As observed in Figure 2, fibers of titer of about 1 dtex (10 μm) were produced with a draw ratio of 20 at an extrusion velocity of 3.5 m/min. By increasing the draw ratio, the cellulose chains are subjected to greater extensional stresses which enhance their alignment. The ordering of the molecules creates a packed network and cohesive forces between neighboring molecules are thus formed. Furthermore, the reduction in temperature of the filament in the air gap leads to an increase in viscosity of the elongated fluid which is further superimposed by the strain-hardening effect of the filament stretch. This rise in viscosity results in an increase of the relaxation time of the cellulose chains which is a phenomenon competing with the orientation process.[21,22,33] As noticed in Figure 2, the total orientation of the resulting fibers become larger by increasing the draw ratio. When stretched, the filament experiences an acceleration of the material accompanied by a reduction in its diameter which results in an increase of the extensional stress within the filament and thus of the molecular orientation.[19] As seen in Figure 2, the orientation of the polymer chains is developed rapidly at

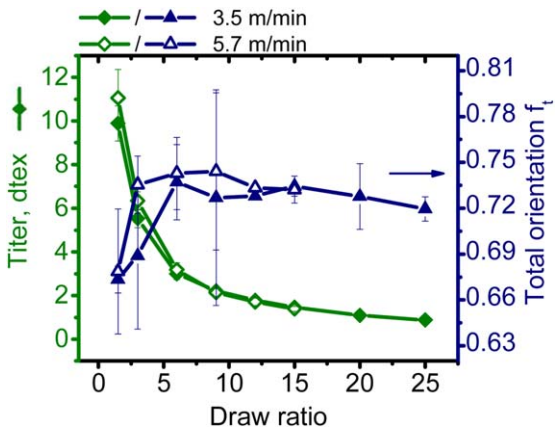

Figure 2. Titer and total orientation as a function of draw ratio at extrusion velocities of 3.5 and 5.7 m/min. [Color figure can be viewed in the online issue, which is available at wileyonlinelibrary.com.]

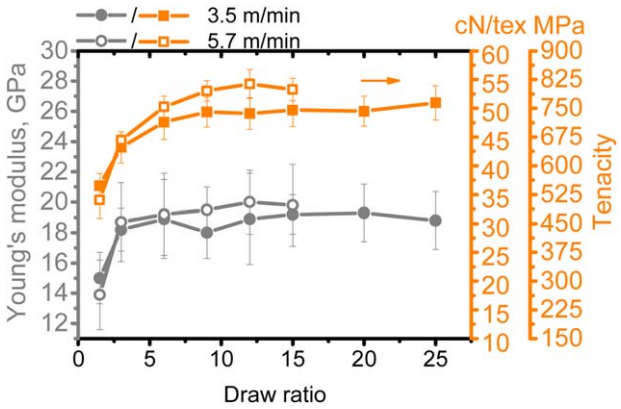

Figure 3. Young's modulus and tenacity as a function of draw ratio at extrusion velocities of 3.5 and 5.7 m/min. [Color figure can be viewed in the online issue, which is available at wileyonlinelibrary.com.]

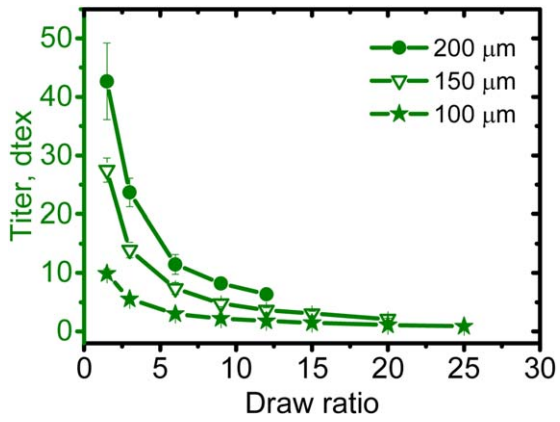

Figure 5. Titer as a function of draw ratio of filaments spun with 100, 150, and 200 µm spinnerets. [Color figure can be viewed in the online issue, which is available at wileyonlinelibrary.com.]

low draws and seems to reach a plateau at a draw of 6, corresponding to a total orientation of about 0.73. At this relatively low draw, the cellulose chains might have already approached their full extension and, hence, their maximum orientation.[21] Only a small draw is thus required to obtain highly orientated cellulose chains. A slight decrease in orientation is noticed after a draw of 15 for the fibers spun at a speed of 3.5 m/min. This small decline might be attributed to chain slippage which is a phenomenon occurring when the polymer chains reach full extension. The morphology of the fibers collected at a draw ratio of 12 has been captured by scanning electron microscopy and is illustrated in Figure 4. A typical smooth fiber surface, round cross-section, and homogeneous and dense fibrillar structure is observed.[18] The results presented in this study are comparable to the ones presented by Mortimer *et al.* on the NMMO-Lyocell fibers.[21] They also revealed that a small draw of about 6 was sufficient to produce highly oriented Lyocell fibers and that chain slippage was occurring at high draw ratios. Figure 2 compares the orientation of cellulose fibers spun at extrusion velocities of 3.5 and 5.7 m/min. Due to technical limitations in the take-up velocity, only a maximum draw of 15 could be set at an extrusion speed of 5.7 m/min whereas a maximum draw of 25 could be reached at a speed of 3.5 m/min. No significant effect of the extrusion velocity on the total orientation of the cellulose chains (Figure 2) and on the Young's modulus (Figure 3) was observed. However, slightly lower tenacities, represented in Figure 3, are obtained at a speed of 3.5 m/min. A similar trend was shown by Jiang *et al.* who explained the superior mechanical properties of the fibers by the augmentation in stress of the spinning line as the spinning speed was increased.[23] On the contrary, Mortimer *et al.* report no significant influence of the spinning speed on the orientation and mechanical properties of Lyocell fibers spun at different speeds.[21] In Figures 2 and 3, the orientation and modulus level off above a draw ratio of about 6 while the tenacity showed a subtle further development. This is in line with our earlier reported results for fibers spun from a 13 wt % eucalyptus prehydrolysis kraft pulp-[DBNH]OAc solution.[34] However, in this study we observed that the development also depends on the polymer concentration of the solution.

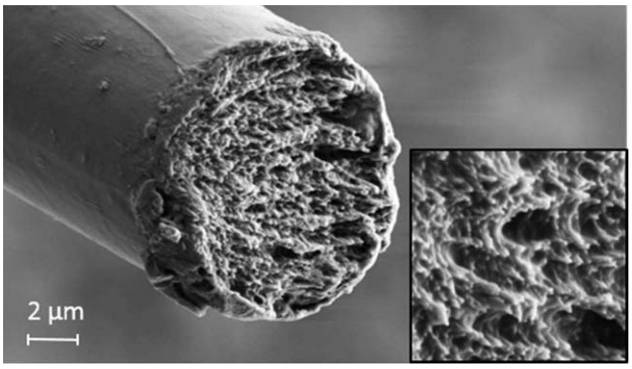

Figure 4. Scanning electron microscopy images of Ioncell-fiber extruded at a velocity of 5.7 m/min and collected at a draw of 12. The inset in the right corner show a 2.5 times magnification of the body of Ioncell fiber.[18]

Influence of the Spinneret Diameter

The spinneret diameter has a significant influence on the filament shape in the air gap and consequently on its intrinsic properties before it enters the coagulation bath. Evidently, the solution throughput and the thickness of the fluid-filament increase with the use of larger diameter spin capillaries. Consequently, higher draw ratios are required to obtain the filaments with the desired titer of 1.2–1.7 dtex. Less efficient cooling of the fluid-filament in the air gap is another result of an increase in diameter as the surface area to volume ratio is reduced. A filament extruded with a 100 µm spinneret presents 100% more relative surface area than a filament extruded with a 200 µm spinneret. Slower cooling causes a diminution in stress within the filament which affects the extension of the polymer chains in the air gap.[19,21,22]

Figure 5 illustrates the decay of the filament fineness extruded at a linear velocity of 3.5 m/min for three different spinneret sizes at increasing draw ratio. The decrease of the titer follows the relation defined by Hauru *et al.* between the titer and the draw ratio.[32] A draw of 2.5 is needed with a 100 µm spinneret to obtain a titer of about 6 dtex (22 µm) whereas with the 150 and 200 µm spinnerets, draws of about 7 and 12, respectively, are required. Higher draw ratio would be needed with the 200

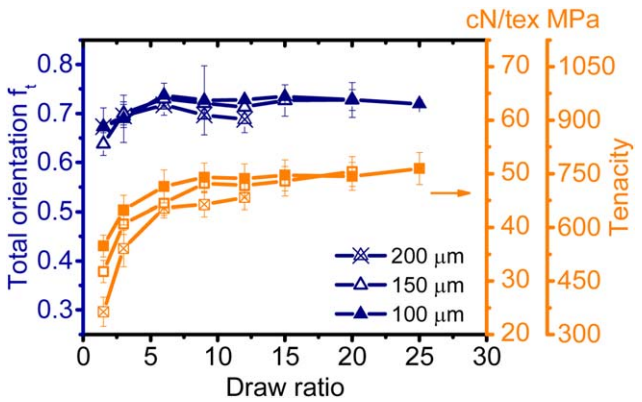

Figure 6. Total orientation and tenacity as a function of draw ratio of filaments spun with 100, 150, and 200 µm spinnerets. [Color figure can be viewed in the online issue, which is available at wileyonlinelibrary.com.]

µm to spin filament with a titer as low as 2 dtex. However, due to the technical limitations of the take-up godet, the maximum draw ratio reachable with the 200 µm spinneret was 12. Figure 6 exhibits the total orientation and tenacity of the fibers spun with the three spinnerets at increasing draw ratios. No significant effect of the spinneret diameter on the cellulose chain orientation is observed. Nevertheless, slightly lower tenacities of the fibers spun with the 200 µm spinneret are observed with a maximum of 46 cN/tex (690 MPa) whereas tenacities of 50 cN/tex (750 MPa) are obtained with the 100 and 150 µm spinnerets. Larger influence of the spinneret diameter on the mechanical properties of Lyocell fibers was detected by Mortimer *et al.*[21]

Determination of the Extensional Viscosity of the Fluid Filament in the Air Gap

At a given molecular weight distribution and solute concentration, the orientation of the cellulose chains during spinning is mainly a result of the drawing process in the air gap. The elongational viscosity of the liquid thread in the air gap undergoes the creation of a certain tension within the filament affecting the fiber structure. A too high tension can induce relaxation effects in the coagulation bath and damage to the filament in the initial stage of precipitation. Boerstoel *et al.* assumed a constant elongational viscosity of solution of cellulose in phosphoric acid in the air gap and a force after the coagulation bath inversely proportional to the air gap length.[35] Figure 7 represents the force acting on the bundle of filaments at the exit of the coagulation bath as a function of the reciprocal air gap length for a solution of 13 wt % extruded at speeds of 3.5, 5.2, and 5.7 m/min with spinnerets of 100 and 150 µm at a draw ratio of 1.5. The elongational viscosities were calculated from the slope according to eq. (4) and are summarized in Table II.

The diameter of the spinneret capillary demonstrates a significant influence on the calculated elongational viscosity. An increase in diameter of 50% results in a drop of about 48.6% in the elongational viscosity. As explained earlier, a wider spinneret capillary corresponds to a larger solution throughput and thus a slower cooling of the fluid filament which undergo a slower rise of the extensional viscosity along the air gap. The extrusion speed seems to have a lower effect on the extensional viscosity. A viscosity of 82,000 Pa s was calculated with a velocity of 5.7 m/min while a value of 96,000 Pa s was obtained with a speed of 3.5 m/min. At lower extrusion velocity, the filaments spend more time in the air gap which also implies more time to cool down, resulting in an increase of the elongational viscosity. Boerstoel reported extensional viscosity between 8200 and 44,600 Pa s for liquid crystalline solutions of cellulose in super phosphoric acid of various concentrations and shear viscosities.[30]

The ratio of the elongational and zero-shear viscosity (Trouton ratio) shows relatively low values, particularly the ratio from the experiment using the 150 µm spinneret. The authors do not have conclusive explanation for these observations. The simplifications on the velocity of the fluid filament in the air gap and the assumptions in the resulting force balance made by Boerstoel might not be valid.[30] Boerstoel neglects the gravitational, surfacial, and inertial forces in the force balance considering them to be small for high viscous materials compared to the external and rheology forces whereas other studies demonstrate the potential importance of these forces in the calculation of the extensional properties of a material.[36,37] Furthermore, the low draw ratio used in these experiments (DR 1.5) results in relatively thick fluid threads in the air gap and may increase the gravitational, inertial, and surfacial effects. Under these conditions, the assumption of neglecting them may not be valid.

The air gap length appears to have no influence on the titer and Young's modulus properties of the resulting fibers, as observed in Table III summarizing the properties of the fibers spun at 3.5 m/min with a 100 µm spinneret and collected at a draw ratio of 1.5. On the other hand, a minor decrease in the tenacity and consequently a slight increase in the elongation is noticed even though the total orientation of the chains does not show a clear decrease with the growth of the air gap length.

Influence of the Coagulation Bath Temperature

The precipitation of dissolved cellulose from IL solutions follows the principles of phase separation in polymer solutions

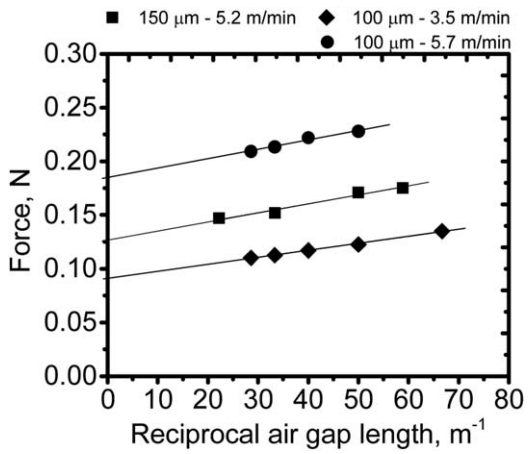

Figure 7. Force after the coagulation bath as a function of reciprocal air gap length for a 13 wt % solution extruded at an extrusion speed of 3.5, 5.2, and 5.7 m/min with 100 and 150 µm spinneret.

Table II. Spinning Parameters, Zero-Shear Viscosity, and Calculated Elongational Viscosity

Spinneret	Extrusion velocity (m/min)	Spinning temperature (°C)	Zero-shear viscosity[a] (Pa s)	Elongational viscosity (Pa s)
36 μm × 150 μm—*L*/*D* 0.2	5.2	76	31,955	42,000
36 μm × 100 μm—*L*/*D* 0.2	3.5	76	27,100	96,000
36 μm × 100 μm—*L*/*D* 0.2	5.7	75	27,868	82,000

[a] Calculated from oscillatory shear measurement.

and starts when the fluid filaments enter the aqueous coagulation bath. Water, which is a polar liquid and miscible with [DBNH]OAc, causes the removal of the solvent from the fluid filaments via an exchange process of solvent against non-solvent. The mechanism of regeneration of cellulose from IL solutions is not yet fully understood. However, as cellulose is directly dissolved in ionic liquid and then precipitated due to solvent exchange, the coagulation kinetics and the precipitation mechanism of cellulose should occur in a similar way as for cellulose-NMMO solutions.[38,39] According to these studies, the non-solvent penetrates inside the fluid-filament faster than the solvent is diffusing out, starting from the filament–water interface. Biganska and Navard demonstrated a diffusion coefficient of water about 10 times larger than the diffusion coefficient of NMMO.[38] The desolvation of cellulose molecules and the structure formation of regenerated cellulose take place when the surrounding of the cellulose chains is approaching pure water. The diffusion constants of water entering and IL exiting a coagulating cellulose/[DBNH]OAc filament have been determined in another study.[40] This phase separation process, which seems to follow spinodal decomposition,[38,41] results in the formation of a rigid layer on the surface of the filament which surrounds a fluid core. The solid–liquid phase boundary moves inward as the filament travels within the aqueous bath causing a continuous decrease of the fluid core diameter. When exiting the coagulation bath, cellulose should be fully regenerated and solid filaments are collected.[20,42] We found earlier that the spin bath geometry used in this study allows for quantitative coagulation at all take-up velocities investigated herein.[40] The regeneration of cellulose from [DBNH]OAc solution was investigated in aqueous bath at different temperatures. The cellulose/[DBNH]OAc solution was subjected to steady shear stress in the spinneret capillary during this experiment as the spinneret diameter (100 μm) and extrusion velocity (5.7 m/min) were kept constant. The bath temperature was gradually increased from 15 to 30 °C and fibers were collected at 15, 20, and 23 °C at draw ratios ranging from 1.5 to 15. Figure 8 exhibits the total orientation and the tenacity of the collected fibers. According to Fink *et al.*, the solvent-exchange process occurs faster than the polymer chain relaxation and thus the chain alignment built in the air gap is preserved and fixated upon the entrance of the fluid filament in the precipitation bath in which the oriented chains interact and crystallize.[7] Mortimer and Peguy stated that further increase in orientation occurs in the coagulation bath due to structural modifications of the material during precipitation and during collapsing at the exit of the bath as water is removed from the filament.[19] The differences in fiber properties observed in Figure 8 are related to the intrinsic response of the oriented cellulose network when the fluid filament enters the aqueous bath of different temperatures as the other parameters were kept constant. The rate of mass transfer and the phase separation process are strongly related to the temperature of the non-solvent. Gavillon and Budtova showed that NMMO release from cellulose solutions into the coagulation bath is quicker at higher bath temperature resulting in faster cellulose regeneration.[39] The fibers regenerated in the 15 °C bath demonstrate a slightly higher total orientation and tenacity than the ones regenerated at 20 and 23 °C. Total orientations and tenacities of about 0.73 and 50 cN/tex (750 MPa), respectively, were achieved at 15 °C whereas total orientations and tenacities of around 0.70 and 45 cN/tex (675 MPa), respectively, were attained at 20 and 23 °C. However, no influence of the bath temperature is

Table III. Tensile Properties of Fibers Spun 13 wt % Solution at 76 °C with a 36 holes, 100 μm, *L*/*D* 0.2 Spinneret at 3.5 m/min

Air gap length (cm)	Titer (dtex)	±	Total orientation	±	Tenacity (cN/tex)	±	Elongation (%)	±	Young's modulus (GPa)	±
1.0	12.2	0.8	0.623	0.020	33.2	1.9	14.8	1.5	14.9	1.8
1.5	12.6	0.6	0.601	0.006	32.0	1.6	17.4	1.2	13.4	1.3
2.0	12.6	0.9	0.618	0.019	29.4	2.0	16.3	1.9	14.1	1.8
2.5	12.6	1.1	0.632	0.022	28.2	2.6	16.6	1.5	13.2	1.5
3.0	12.6	1.2	0.659	0.019	28.5	2.3	18.4	1.6	13.1	1.4
3.5	12.4	1.2	0.583	0.023	28.2	2.5	18.4	2.8	13.9	2.2

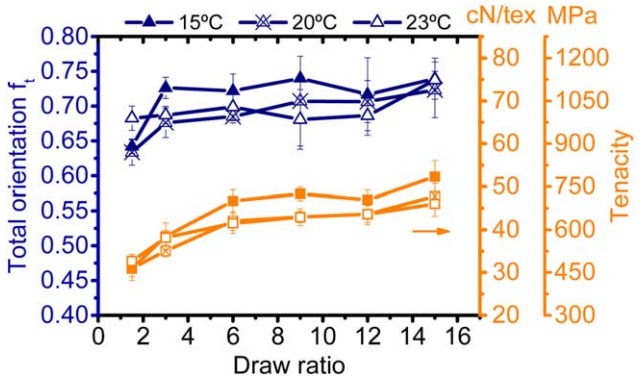

Figure 8. Total orientation and tenacity as a function of draw ratio of filaments coagulated in water at 15, 20, and 23 °C. [Color figure can be viewed in the online issue, which is available at wileyonlinelibrary.com.]

seen at a draw of 1.5. It might be explained by the moderate orientation of the cellulose chains occurring in the air gap at that draw. The effect of chain relaxation in the spin bath is thus low. The collection of filament was impossible with a coagulation bath of temperature higher than 25 °C due to the constant breaks of the filaments occurring in the bath even at very low draw. These failures might exist due to the skin-core (solid-liquid) structure of the filament. Indeed the tension generated within the filament during drawing is transmitted to the solid–liquid boundary which might fail if the tension becomes too prominent. A potential mechanism is the detachment of the liquid region of the filament through a telescopic type motion.[20,42] Lowering the temperature of the bath may cause the development of a stronger liquid core which may show more resistance toward deformation. By rising the temperature of the coagulation bath, the maximum stress tolerated by the liquid-core structure is getting smaller and breaks are favored. One explanation for this phenomenon, adapted from Lindman and coworkers, could be the presence of more polar states of the cellulose molecules which might originate from conformational changes at low temperature. The formation of a stronger liquid core at lower temperature might indicate the more numerous polar–polar interactions due to the more populated polar states.[43]

CONCLUSIONS

This article reveals the effect of the spinneret diameter, extrusion velocity, draw ratio, and coagulation bath temperature on the formation of the cellulose molecular structure and on the mechanical properties of the dry filament.

At the given polymer concentration, we demonstrated that a draw ratio of about 6 was sufficient for the formation of a highly oriented cellulose network which ensures the production of high tenacity fibers. The increase of the extrusion velocity establishing a rise in the shear stress in the spinneret capillary favored slightly superior tenacity. It was also shown that the reduction of the spinneret capillary diameter contributes to the increase in stress within the filament in the air gap enlarging the extension of the cellulose chains and hence the tenacity of the spun fibers. The increase of the coagulation bath temperature to room temperature caused the constant failure of the filament in the bath preventing the collection of fibers. Lowering the temperature strengthened the nascent filament in the water bath which allowed for the necessary stress transfer through the coagulation zone to the air gap where the liquid filaments are elongated.

Furthermore, radial force measurement of the filaments at the exit of the coagulation bath for the determination of the elongational viscosity appeared to be an appropriate method and showed promising results. Further investigation with particular emphasis on the effect of the cellulose concentration is necessary to better understand the effect of elongational stress on the structure formation.

ACKNOWLEDGMENTS

This study is part of the *Future Biorefinery* and *Advanced Cellulose to Novel Products* programs financed by the Finnish Bioeconomy Cluster (FIBIC) and the Finnish Funding Agency for Innovation (TEKES).

REFERENCES

1. Eichinger, D. *Chem. Fibers Int.* **2011**, *61*, 177.
2. Haemmerle, F. M. *Lenzinger Ber.* **2011**, *89*, 12.
3. Woodings, C. Regenerated Cellulose Fibres; Woodhead Publishing Limited: Cambridge, England, **2001**.
4. Shen, L.; Patel, M. K. *Lenzinger Ber.* **2010**, *88*, 1.
5. Coulsey, H. A.; Smith, S. B. *Lenzinger Ber.* **1995**, *75*, 51.
6. Eichinger, D.; Eibl, M. *Lenzinger Ber.* **1995**, *75*, 41.
7. Fink, H. P.; Weigel, P.; Purz, H.; Ganster, J. *Prog. Polym. Sci.* **2001**, *26*, 1473.
8. Perepelkin, K. *Fibre Chem.* **2007**, *39*, 163.
9. Hermanutz, F.; Gähr, F.; Uerdingen, E.; Meister, F.; Kosan, B. *Macromol. Symp.* **2008**, *262*, 23.
10. Feng, L.; Chen, Z. *J. Mol. Liq.* **2008**, *142*, 1.
11. Swatloski, R. P.; Rogers, R. D.; Holbrey, J. D. U.S. Patent 0157351 A1 (**2003**).
12. Pinkert, A.; Marsh, K. N.; Pang, S.; Staiger, M. P. *Chem. Rev.* **2009**, *109*, 6712.
13. Cao, Y.; Wu, J.; Zhang, J.; Li, H.; Zhang, Y.; He, J. *Chem. Eng. J.* **2009**, *147*, 13.
14. Mäki-Arvela, P.; Anugwom, I.; Virtanen, P.; Sjöholm, R.; Mikkola, J. *Ind. Crops Prod.* **2010**, *32*, 175.
15. Wendler, F.; Kosan, B.; Krieg, M.; Meister, F. *Macromol. Symp.* **2009**, *280*, 112.
16. Hummel, M.; Michud, A.; Tanttu, M.; Asaadi, S.; Ma, Y.; Hauru, L. K.; Parviainen, A.; King, A. W.; Kilpeläinen, I.; Sixta, H. *Adv. Polym. Sci.* **2016**, *271*, 133.
17. Michud, A.; King, A.; Parviainen, A.; Sixta, H.; Hauru, L.; Hummel, M.; Kilpeläinen, I. WO Patent 162062 A1 (**2014**).
18. Michud, A.; Tanttu, M.; Asaadi, S.; Ma, Y.; Netti, E.; Kääriainen, P.; Persson, A.; Berntsson, A.; Hummel, M.; Sixta, H. *Text. Res. J.* **2016**, *86*, 543.

19. Mortimer, S.; Peguy, A. *Cellulose Chem. Technol.* **1996**, *30*, 117.
20. Ziabicki, A. Fundamentals of Fibre Formation; Wiley: USA; **1976**.
21. Mortimer, S.; Peguy, A.; Ball, R. *Cellulose Chem. Technol.* **1996**, *30*, 251.
22. Mortimer, S.; Peguy, A. *J. Appl. Polym. Sci.* **1996**, *60*, 1747.
23. Jiang, G.; Yuan, Y.; Wang, B.; Yin, X.; Mukuze, K. S.; Huang, W.; Zhang, Y.; Wang, H. *Cellulose* **2012**, *19*, 1075.
24. Berggren, R.; Berthold, F.; Sjöholm, E.; Lindström, M. *J. Appl. Polym. Sci.* **2003**, *88*, 1170.
25. Borrega, M.; Tolonen, L. K.; Bardot, F.; Testova, L.; Sixta, H. *Bioresour. Technol.* **2013**, *135*, 665.
26. Hauru, L. K.; Ma, Y.; Hummel, M.; Alekhina, M.; King, A. W.; Kilpeläinen, I.; Penttilä, P. A.; Serimaa, R.; Sixta, H. *RSC Adv.* **2013**, *3*, 16365.
27. Sammons, R.; Collier, J.; Rials, T.; Petrovan, S. *J. Appl. Polym. Sci.* **2008**, *110*, 1175.
28. Lu, F.; Cheng, B.; Song, J.; Liang, Y. *J. Appl. Polym. Sci.* **2012**, *124*, 3419.
29. Michud, A.; Hummel, M.; Sixta, H. *Polymer* **2015**, *75*, 1.
30. Boerstoel, H. Liquid Crystalline Solutions of Cellulose in Phosphoric Acid for Preparing Cellulose Yarns; Ph.D. Thesis, Rijksuniversiteit Groninnen, May **1998**.
31. Adusumalli, R.; Keckes, J.; Martinschitz, K. J.; Boesecke, P.; Weber, H.; Roeder, T.; Sixta, H.; Gindl, W. *Cellulose* **2009**, *16*, 765.
32. Hauru, L. K.; Hummel, M.; Michud, A.; Sixta, H. *Cellulose* **2014**, *21*, 4471.
33. Golzar, M. Melt Spinning of the Fine Peek Filaments; Ph.D Thesis, June **2004**.
34. Sixta, H.; Michud, A.; Hauru, L.; Asaadi, S.; Ma, Y.; King, A. W.; Kilpelainen, I.; Hummel, M. *Nordic Pulp Paper Res. J.* **2015**, *30*, 43.
35. Boerstoel, H.; Maatman, H.; Westerink, J.; Koenders, B. *Polymer* **2001**, *42*, 7371.
36. Szabo, P. *Rheol. Acta* **1997**, *36*, 277.
37. Szabo, P.; McKinley, G. H. *Rheol. Acta* **2003**, *42*, 269.
38. Biganska, O.; Navard, P. *Biomacromolecules* **2005**, *6*, 1948.
39. Gavillon, R.; Budtova, T. *Biomacromolecules* **2007**, *8*, 424.
40. Hauru, L. K.; Hummel, M.; Nieminen, K.; Michud, A.; Sixta, H. *Soft Matter* **2016**, *12*, 1487.
41. Eckelt, J.; Eich, T.; Röder, T.; Rüf, H.; Sixta, H.; Wolf, B. A. *Cellulose* **2009**, *16*, 373.
42. Paul, D. *J. Appl. Polym. Sci.* **1968**, 12, 2273.
43. Medronho, B.; Romano, A.; Miguel, M. G.; Stigsson, L.; Lindman, B. *Cellulose* **2012**, *19*, 581.